Bond graph – based filtered inversion of multivariable physical systems

R F Ngwompo

Centre for Power Transmission and Motion Control

Department of Mechanical Engineering, University of Bath, Bath, BA2 7AY, UK.

Email: R.F.Ngwompo@bath.ac.uk

Abstract: In a variety of fields, system inversion is often required in order to determine inputs from measured or for desired outputs. However, inverse systems are often non-proper in the sense that they require differentiators in their realisation. This leads to numerical difficulties associated with the computer implementation of their mathematical models. To overcome these problems, approximate inversion also referred to as filtered inversion is proposed for systems modelled by bond graphs. Generic configurations of right and left filtered inverse bond graph models are proposed with dynamic structural conditions on the filters so that the resulting composite bond graph represents a proper system suitable for effective numerical implementations.

Keywords: bond graph, inversion, filtered inverse, approximate inversion, essential orders.

1. INTRODUCTION

Inverse systems have received a great deal of attention over the years since the pioneering research work in this area published in the 60s (see for e.g. references [**1-3**] to name a few). System inversion appears not only implicitly in many control problems such as feedforward control and decoupling problems [**4**], iterative learning control [**5**] but also as an explicit problem whenever the determination of control actions associated with measured or pre-specified outputs are required (e.g. actuator sizing [**6**], flight trajectory planning [**7**]). However, inverse systems are known to be often non-proper or noncausal in the sense that they require differentiators for their realisation. This leads to numerical difficulties associated with the computer implementation of their mathematical models. To overcome these problems, the idea of filtered inverse was proposed by Yoshikawa and Sugie [**8**] as a type of approximate inverse systems that are proper (not requiring differentiators) and able to reproduce input from output in a certain frequency range. Following the work of Yoshikawa and Sugie presented using the transfer function approach, state-space methods to the filtered inverse problem have been proposed by Yamada *et al* [**9**].

Strictly speaking, there are two types of inversion problems: (i) left inverse which computes the inputs from measured outputs and (ii) right inverse which determines the inputs required to achieve some desired outputs. Both left and right inverses may exist only when a system has the same number of inputs as outputs, and in this case both inverse models are identical and left and right inversion problems need not be considered separately. However, as will be shown in this paper, in the case of invertible systems with identical number of inputs and outputs, there are some differences between right and left filtered inversion that depend on the input-output structure of the system.

Bond graph modelling technique [**10**, **11**], also developed in the 60s has increasingly been used for modelling and analysis of physical systems. Bond graphs provide a unified graphical representation of multi-domain engineering systems that enables models structural analysis i.e. properties not depending on numerical parameters on the one hand and automatic generation of mathematical models associated with various system analysis problems using the concept of causality and its generalisation to bicausality [**12, 13**] on the other hand. Inverse models and their applications in control systems design have previously been considered using bond graph representation [**14**]. In general, these exact inverse bond graph models and the associated mathematical models can hardly be implemented numerically for the reasons cited above.

In this paper, a bond graph approach to filtered inversion of multivariable systems is proposed as an alternative to exact inverse bond graph models. It is shown that a composite bond graph configuration combining filters (or specification models) and actual system model can conveniently represents a filtered inverse bond graph model that is proper provided that the filters satisfy some appropriate structural dynamic properties that will be stated. The advantage of using bond graphs for such a problem is that the methodology is a physical-model based approach that can be extended to nonlinear systems modelled by bond graphs. The results presented here can be considered as an extension of the bond graph-based simulation of nonlinear inverse systems using physical performance specifications previously proposed in [**15**]. The mathematical model generated from the proposed filtered inverse bond graph can therefore be implemented as a numerically more robust although approximate inverse model in various control system design problems requiring system inversion.

In the context of feedback control systems, "high gains" are commonly used for approximate inversion or estimation of state variables through observers. Thus, the proposed inversion methodology is closely related to "high gains" as both techniques deal with approximating non-proper dynamical systems (i.e. with differentiators) by dynamical systems that are proper. Such approximation problem has also been considered in the design of proper control law by Bonilla *et al* [**16**] (see also [**17**]). A contribution of the present paper is to present a general

framework for the filtered inversion problem using the structural properties of bond graphs and their associated physical interpretation. However, the problem of assigning the systems parameters or their relative values for better approximation such as expressed by "high gains" is not discussed in general but rather considered on an illustrative example that is developed later in the paper.

In section 2, generic concepts of inverse and filtered inverse systems as well as some related input-output structural properties are recalled. Section 3 presents a bond graph interpretation of the concepts introduced in section 2 and build on the graphical properties to propose a bond graph based configuration to represent left and right filtered inverse models. The generation of mathematical models from filtered inverse bond graphs and the symbolic manipulations leading to appropriate state space forms are also discussed in section 3. An illustrative example is provided in section 4 and issues related to the proposed technique as well as its extension to nonlinear models are discussed in section 5. Section 6 concludes the paper.

2. INVERSE AND FILTERED INVERSE SYSTEMS

Consider a square system (same number of inputs and outputs) described by its state space model

$$\begin{aligned} \dot{\boldsymbol{x}}(t) &= \mathbf{A}\boldsymbol{x}(t) + \mathbf{B}\boldsymbol{u}(t) \\ \boldsymbol{y}(t) &= \mathbf{C}\boldsymbol{x}(t) + \mathbf{D}\boldsymbol{u}(t) \end{aligned} \;;\; \boldsymbol{x}(0) = 0 \tag{1}$$

where $\boldsymbol{u} \in R^m$ is the input vector, $\boldsymbol{y} \in R^m$ is the output vector, $\boldsymbol{x} \in R^n$ represents the state vector and the matrices $\mathbf{A}$, $\mathbf{B}$, $\mathbf{C}$ and $\mathbf{D}$ are of appropriate dimensions. The transfer function of this system is given by

$$\boldsymbol{Y}(s) = \mathbf{G}(s)\,\boldsymbol{U}(s) \tag{2}$$

where $$\mathbf{G}(s) = \mathbf{C}\left(s\mathbf{I} - \mathbf{A}\right)^{-1}\mathbf{B} + \mathbf{D} \tag{3}$$

When the system is invertible, its inverse model can be written in the minimal-order (lowest possible dynamic order) form [**2**, **4**]

$$\begin{cases} \dot{\boldsymbol{z}}(t) = \overline{\mathbf{A}}\,\boldsymbol{z}(t) + \overline{\mathbf{B}}(p)\,\boldsymbol{y}(t) \\ \boldsymbol{u}(t) = \overline{\mathbf{C}}\,\boldsymbol{z}(t) + \overline{\mathbf{D}}(p)\,\boldsymbol{y}(t) \end{cases} \tag{4}$$

where $\boldsymbol{z}$ is the inverse model state r-dimensional vector ($r \le n$); $\overline{\mathbf{A}}$ and $\overline{\mathbf{C}}$ are constant matrices of appropriate dimensions ; $\overline{\mathbf{B}}(p)$ and $\overline{\mathbf{D}}(p)$ are polynomial matrices in the differential operator $p \triangleq d/dt$.

The minimal inverse model (4) may be obtained using Silverman's classical inversion algorithm that starts with the state space model (1) and consists of a sequence of algebraic row operations and differentiations on the output vector $\boldsymbol{y}(t)$ to solve the inputs in terms of the output components, followed by an appropriate state transformation [**2**]. Alternatively, with the transfer-function approach, the minimal inverse model may be constructed as a space-state realisation of the irreducible form of the inverse of the transfer function (3) [**4**]. Either way, it is clear from (4) that the realisation of the inverse model requires various derivatives of the output components $y_1(t), y_2(t), \cdots, y_m(t)$. Denoting α_i; $i = 1, 2, \cdots, m$, the highest derivative order required for the output component $y_i(t)$, it is shown that $\alpha_i \le n$ where n is the order of the original forward system [**2**].

From the numerical implementation viewpoint, differentiators in the inverse model are not desirable in general. A technique to avoid differentiators is to reconstruct approximate input through filtered inverse models that are proper or causal. Using the transfer matrix representation (3), the following definitions are given.

Definition 1[**8**]

A *left filtered inverse* system, when it exists, may be defined by its proper rational matrix $\mathbf{G}_{\mathrm{LF}}(s)$ such that

$$\mathbf{G}_{\mathrm{LF}}(s)\,\mathbf{G}(s) = \mathbf{Q}_{\mathrm{LF}}(s) \tag{5}$$

where $$\mathbf{Q}_{\mathrm{LF}}(s) = \mathrm{diag}\left\{(T_1 s+1)^{-\alpha_{\mathrm{L}1}}\ (T_2 s+1)^{-\alpha_{\mathrm{L}2}}\ \cdots\ (T_m s+1)^{-\alpha_{\mathrm{L}m}}\right\} \tag{6}$$

$T_i > 0$; $i = 1, 2, \cdots, m$ are chosen constants

and $\alpha_{\mathrm{L}i}$; $i = 1, 2, \cdots, m$ are non-negative integers

Definition 2

In a similar manner, a *right filtered inverse* system, when it exists, may be defined by its proper rational matrix $\mathbf{G}_{\mathrm{RF}}(s)$ such that

$$\mathbf{G}(s)\,\mathbf{G}_{\mathrm{RF}}(s) = \mathbf{Q}_{\mathrm{RF}}(s) \tag{7}$$

where $$\mathbf{Q}_{\mathrm{RF}}(s) = \mathrm{diag}\left\{(T_1 s+1)^{-\alpha_{\mathrm{R}1}}\ (T_2 s+1)^{-\alpha_{\mathrm{R}2}}\ \cdots\ (T_m s+1)^{-\alpha_{\mathrm{R}m}}\right\} \tag{8}$$

$T_i > 0$; $i = 1, 2, \cdots, m$ are chosen constants

and $\alpha_{\mathrm{R}i}$; $i = 1, 2, \cdots, m$ are non-negative integers

Remark1

In the above definitions, the terms $(T_i s+1)^{-\alpha_{\mathrm{L}i}}$ (resp. $(T_i s+1)^{-\alpha_{\mathrm{R}i}}$) are chosen for simplicity and any of these can be replaced by any rational function whose relative degree is greater than or equal to $\alpha_{\mathrm{L}i}$ (resp. $\alpha_{\mathrm{R}i}$). Hence it is obvious that filtered inverses are not unique and depend on the choice of the filters.

Right or left filtered inverses above can be interpreted as cascading the inverse model with pre- or post-filters of appropriate orders to obtain proper dynamic systems that shape or approximately reconstruct the inputs over some frequency range defined by the constants $T_i > 0$ or the parameters of any alternative rational function replacing $(T_i s+1)^{-\alpha_{\mathrm{L}i}}$ or $(T_i s+1)^{-\alpha_{\mathrm{R}i}}$. In order to achieve this, the filters must have appropriate structural dynamic properties, in particular, each relative degree $\alpha_{\mathrm{L}i}$ in $\mathbf{Q}_{\mathrm{LF}}(s)$ (resp. $\alpha_{\mathrm{R}i}$ in $\mathbf{Q}_{\mathrm{RF}}(s)$) should be at least equal to a specific minimum value $\overline{\alpha}_{\mathrm{L}i}$ (resp. $\overline{\alpha}_{\mathrm{R}i}$) uniquely determined by the input-output structure of the system:

$$\alpha_{\mathrm{L}i} \geq \overline{\alpha}_{\mathrm{L}i};\ i=1,2,\cdots,m \tag{9}$$

resp.
$$\alpha_{\mathrm{R}i} \geq \overline{\alpha}_{\mathrm{R}i};\ i=1,2,\cdots,m \tag{10}$$

The minimum values $\overline{\alpha}_{\mathrm{L}i};\ i=1,2,\cdots,m$ such that a left inverse system $\mathbf{G}_{\mathrm{LF}}(s)$ that is proper and satisfying (5) exists, are related to the "L-integral" inverse introduced by Sain and Massey [**3**] and subsequently extended to the minimal "$[\alpha_1, \alpha_2, \cdots \alpha_m]-$ left integral" inverse by Kamiyama and Furuta [**18**]. From the discrete system associated with the system (1), the series of $(k+1)m\times(k+1)m$ matrices $\mathbf{M}_k$ that relate the sequence of the k inputs segments $\boldsymbol{u}_{[0,k]}=[\boldsymbol{u}(k)^{\mathrm{T}}\ \cdots\ \boldsymbol{u}(1)^{\mathrm{T}}\ \boldsymbol{u}(0)^{\mathrm{T}}]^{\mathrm{T}}$ to the sequence of k outputs segments $\boldsymbol{y}_{[0,k]}=[\boldsymbol{y}(k)^{\mathrm{T}}\ \cdots\ \boldsymbol{y}(1)^{\mathrm{T}}\ \boldsymbol{y}(0)^{\mathrm{T}}]^{\mathrm{T}}$ so that $\boldsymbol{y}_{[0,k]}=\mathbf{M}_k\boldsymbol{u}_{[0,k]}$ are defined as follows [**3**]:

$$\mathbf{M}_0=[\mathbf{D}],\qquad \mathbf{M}_k=\begin{bmatrix}\mathbf{D} & \mathbf{CB} & \mathbf{CAB} & \cdots & \mathbf{CA}^{k-1}\mathbf{B}\\ \mathbf{0} & \mathbf{D} & \mathbf{CB} & \cdots & \vdots\\ \vdots & \mathbf{0} & \mathbf{D} & \cdots & \vdots\\ \vdots & \vdots & \vdots & \ddots & \mathbf{CB}\\ \mathbf{0} & \mathbf{0} & \mathbf{0} & \ddots & \mathbf{D}\end{bmatrix} \tag{11}$$

The following results are recalled.

Theorem 1 [**8**]

There exists a filtered inverse system for a given system (1) if and only if the system (1) is invertible.

Theorem 2 [**3**]

The system (1) is invertible if and only if

$$\operatorname{rank}\mathbf{M}_n - \operatorname{rank}\mathbf{M}_{n-1} = m \tag{12}$$

Denoting $\mathbf{M}_k(i)$ the $(k+1)m\times((k+1)m-1)$ matrix obtained by eliminating the *i*-th column from $\mathbf{M}_k$, the minimum values $\bar{\alpha}_{\mathrm{L}i}$; $i=1,2,\cdots,m$ in (9) can be determined using the following theorem.

Theorem 3 [**18**]

When the system (1) is invertible (i.e. $\operatorname{rank}\mathbf{M}_n - \operatorname{rank}\mathbf{M}_{n-1} = m$ from Theorem 2),

let

$$\alpha_{\mathrm{L}} = \min\left\{\alpha \mid \operatorname{rank}\mathbf{M}_\alpha - \operatorname{rank}\mathbf{M}_{\alpha-1} = m\right\} \tag{13}$$

$$\bar{\alpha}_{\mathrm{L}i} = \min\left\{\beta \mid \operatorname{rank}\mathbf{M}_{\alpha_{\mathrm{L}}} - \operatorname{rank}\mathbf{M}_{\alpha_{\mathrm{L}}}(\beta m+i) = 1\right\}\ i=1,2,\cdots,m \tag{14}$$

Then the system (1) is $[\alpha_{\mathrm{L}1}, \alpha_{\mathrm{L}2}, \cdots \alpha_{\mathrm{L}m}]$– integral left invertible if and only if $\alpha_{\mathrm{L}i} \ge \bar{\alpha}_{\mathrm{L}i}$, $i=1,2,\cdots,m$.

Although the minimal integral right inversion is not presented in [**18**], the result below is stated and can be proven in a similar manner as for the left inversion. Denoting $\overline{\mathbf{M}}_k(i)$ the $((k+1)m-1)\times(k+1)m$ matrix obtained by eliminating the *i*-th row from $\mathbf{M}_k$, the minimum values $\bar{\alpha}_{\mathrm{R}i}$; $i=1,2,\cdots,m$ are determined by the following theorem.

Theorem 4

When the system (1) is invertible (i.e. $\operatorname{rank}\mathbf{M}_n - \operatorname{rank}\mathbf{M}_{n-1} = m$ from Theorem 2),

let

$$\alpha_{\mathrm{R}} = \min\left\{\alpha \mid \operatorname{rank}\mathbf{M}_\alpha - \operatorname{rank}\mathbf{M}_{\alpha-1} = m\right\} \tag{15}$$

$$\bar{\alpha}_{\mathrm{R}i} = \min\left\{\beta \mid \operatorname{rank}\mathbf{M}_{\alpha_{\mathrm{R}}} - \operatorname{rank}\overline{\mathbf{M}}_{\alpha_{\mathrm{R}}}\left((\alpha_{\mathrm{R}}+1)m-(\beta+1)m+i\right)\right) = 1\right\};\ i=1,2,\cdots,m \tag{16}$$

Then the system (1) is $[\alpha_{\mathrm{R}1}, \alpha_{\mathrm{R}2}, \cdots \alpha_{\mathrm{R}m}]$– integral right invertible if and only if $\alpha_{\mathrm{R}i} \ge \bar{\alpha}_{\mathrm{R}i}$, $i=1,2,\cdots,m$.

Remark 2

In (16), the elimination process of the rows in order to determine $\bar{\alpha}_{\mathrm{R}i}$ starts from the last rows of the matrix $\mathbf{M}_{\alpha_{\mathrm{R}}}$ as the format of the series of matrices is kept as given in (11). It is however possible to rearrange these matrices as in [**3, 19**] so that the elimination process starts from the first row.

In a study on the feedback decoupling problem, known to be linked to right invertibility, Commault et al [**19**] introduced the essential orders of the outputs in relation to the concept of "rank essential" rows proposed by Cremer [**20**]. The duality between right and left inversion is used here to introduce the essential orders of the inputs and highlight the interpretation of these integers in the context of right and left inverse systems.

Definition 3[**20**]

For a given matrix $\mathbf{W}$, the *i*-th row $\boldsymbol{w}_{\mathrm{r}i}$ (resp. the *i*-th column $\boldsymbol{w}_{\mathrm{c}i}$) is said to be *essential* if $\boldsymbol{w}_{\mathrm{r}i}$ (resp. $\boldsymbol{w}_{\mathrm{c}i}$) is not linearly dependent of other rows (resp. other columns). This means that the *i*-th row $\boldsymbol{w}_{\mathrm{r}i}$ (resp. the *i*-th column $\boldsymbol{w}_{\mathrm{c}i}$) cannot be written as a linear combination of other rows (resp. other columns) of $\mathbf{W}$.

Definition 3 implies that eliminating an essential row or column from a square matrix will decrease its rank by a unit. Therefore from the structure of the $\mathbf{M}_k$ matrices defined in (11), equation (14) in Theorem 3 can be rewritten as:

$$\bar{\alpha}_{\mathrm{L}i} = \min\left\{\beta \;\middle|\; \left[(\mathbf{C}\mathbf{A}^{\beta-1}\boldsymbol{b}_i)^{\mathrm{T}} \;\cdots\; (\mathbf{C}\boldsymbol{b}_i)^{\mathrm{T}} \;\; \boldsymbol{d}_i^{\mathrm{T}} \;\; \mathbf{0}^{\mathrm{T}} \;\cdots\; \mathbf{0}^{\mathrm{T}}\right]^{\mathrm{T}} \text{ is an essential column in } \mathbf{M}_{\alpha_{\mathrm{L}}}\right\};\; i=1,2,\cdots,m \quad (17)$$

where $\boldsymbol{b}_i$ and $\boldsymbol{d}_i$ are the *i*-th columns of the matrices $\mathbf{B}$ and $\mathbf{D}$ respectively and superscript T denotes the matrix transpose.

Similar to the left integral inversion, an alternative expression to (16) for $\bar{\alpha}_{\mathrm{R}i}$ in Theorem 4 is as follows:

$$\bar{\alpha}_{\mathrm{R}i} = \min\left\{\beta \;\middle|\; \left[\mathbf{0} \;\cdots\; \mathbf{0} \;\; \bar{\boldsymbol{d}}_i \;\; (\bar{\boldsymbol{c}}_i\mathbf{B}) \;\cdots\; (\bar{\boldsymbol{c}}_i\mathbf{A}^{\beta-1}\mathbf{B})\right]^{\mathrm{T}} \text{ is an essential column in } \mathbf{M}_{\alpha_{\mathrm{R}}}\right\};\; i=1,2,\cdots,m \qquad (18)$$

where $\bar{\boldsymbol{c}}_i$ and $\bar{\boldsymbol{d}}_i$ are the *i*-th rows of the matrices $\mathbf{C}$ and $\mathbf{D}$ respectively.

Definition 5 [**19**]

If the system (1) is right invertible, the integer $\bar{\alpha}_{\mathrm{R}i}$ given by (16) or (18) is called the *essential order of the i-th output* y_i.

In a similar way, the following definition is given.

Definition 4

If the system (1) is left invertible, the integer $\overline{\alpha}_{\mathrm{L}i}$ given by (14) or (17) will be referred to as the *essential order of the i-th input* u_i.

Because the systems considered in this paper are square systems (i.e. with same number m of inputs as outputs), if the system is invertible, both right and left inverses exist, are identical with the integers α_{L} and α_{R} defined in (13) and (15) being obviously identical. The integer α_{L} is called the inherent integration by Sain and Massey [**3**] in their proposed "*L*-integral" inverse systems that reproduce the *L*-th integral of the inputs to the original system. The minimum integral inverse by Kamiyama and Furuta [**18**] defines a tighter version of this concept where the "$[\alpha_{\mathrm{L}1}, \alpha_{\mathrm{L}2}, \cdots \alpha_{\mathrm{L}m}]$– integral" left inverse system outputs are the $\alpha_{\mathrm{L}i}$-th integral of each input u_i to the original system. An interpretation of the inherent integration is that any realisation of the inverse of (1) requires α_{L} derivatives of at least one component of the output [**2**]. In a similar way, the definition of the $[\alpha_{\mathrm{L}1}, \alpha_{\mathrm{L}2}, \cdots \alpha_{\mathrm{L}m}]$– integral left inverse system implies that the reconstruction of each input u_i requires $\alpha_{\mathrm{L}i}$ derivatives of at least one component of the output.

For square invertible systems, denoting $\alpha_{\mathrm{LR}} = \alpha_{\mathrm{L}} = \alpha_{\mathrm{R}}$, the sequence of α_{LR} input-output segments are related by the equation

$$\boldsymbol{y}_{[0,\alpha_{\mathrm{LR}}]} = \mathbf{M}_{\alpha_{\mathrm{LR}}} \boldsymbol{u}_{[0,\alpha_{\mathrm{LR}}]} \tag{19}$$

where $$\boldsymbol{u}_{[0,\alpha_{\mathrm{LR}}]} = [\boldsymbol{u}(\alpha_{\mathrm{LR}})^{\mathrm{T}} \ \cdots \ \boldsymbol{u}(1)^{\mathrm{T}} \ \ \boldsymbol{u}(0)^{\mathrm{T}}]^{\mathrm{T}} \tag{20}$$

$$\boldsymbol{y}_{[0,\alpha_{\mathrm{LR}}]} = [\boldsymbol{y}(\alpha_{\mathrm{LR}})^{\mathrm{T}} \ \cdots \ \boldsymbol{y}(1)^{\mathrm{T}} \ \ \boldsymbol{y}(0)^{\mathrm{T}}]^{\mathrm{T}} \tag{21}$$

and the matrix $\mathbf{M}_{\alpha_{\mathrm{LR}}}$ as defined by (11)

Recalling that the "delay" inverse problem or the associated "integral" inverse problem consists in solving (19) for $\boldsymbol{u}(0)$ [**21**], the definition of the minimum values $\overline{\alpha}_{\mathrm{R}i}$; $i = 1,2,\cdots,m$ in terms of essential rows in the matrix $\mathbf{M}_{\alpha_{\mathrm{LR}}}$ corresponds for each output y_i to the selection of the linearly independent row associated with the minimal delay (or minimum number of integrations) of this output required to solve the integral inverse problem. As for the minimum values $\overline{\alpha}_{\mathrm{L}i}$; $i = 1,2,\cdots,m$ associated with essential columns of the matrix $\mathbf{M}_{\alpha_{\mathrm{LR}}}$, these

indicate for each input u_i, the minimal delay required to reconstruct this input from the outputs in the integral inverse problem. These observations lead to the following properties for the inverse systems.

Property 1

In the left inverse model, when it exists, the essential order $\bar{\alpha}_{\mathrm{L}i}$ of the *i*-th input component $u_i(t)$ as defined by (14) or (17) is the highest derivative of at least one component of the output appearing in the reconstruction of the *i*-th input component $u_i(t)$.

Property 2 [**22**]

In the right inverse model, when it exists, the essential order $\bar{\alpha}_{\mathrm{R}i}$ of the *i*-th output component $y_i(t)$ as defined by (16) or (18) is the highest derivative of the *i*-th output component $y_i(t)$ in the inverse model i.e. required for the determination of all input components.

Properties 1 and 2 above indicate the number of differentiators required for the realisation of left or right inverses and this justifies the structural properties (9) and (10) which the filters must satisfy for the filtered inverse to be proper dynamical systems. A bond graph approach to this problem is presented in the next section.

3. BOND GRAPH APPROACH TO FILTERED INVERSION

3.1 Bond graph based inversion

A necessary and sufficient condition for a filtered inverse system to exist is obviously that the inverse system exists. Bond graph based inversion presented in [**14**] uses the length of causal paths in the forward model[1] to determine the inverse model when it exists.

Definition 5 [**14**]

In the forward bond graph model, the length $l(p)$ of an input-output causal path p is defined as $l(p) \triangleq n_{\mathrm{I}}(p) - n_{\mathrm{D}}(p)$, where $n_{\mathrm{I}}(p)$ (resp. $n_{\mathrm{D}}(p)$) is the number of energy storage elements in integral (resp. derivative) causality met when following the path p. This number determines the net number of integration between the input and the output.

[1] Some authors also refer to "forward model" as "direct model"

The model inversion procedure is summarised below in the following three steps:

(i) Determination of a minimal-length set of disjoint input-output causal paths in the forward model. If no set of disjoint input-output causal paths exist then the system is not invertible and the procedure ends.

(ii) Propagation of the bicausal information from the output **SS** elements to the associated input **SS** elements along the power lines associated with the minimal-length set of disjoint input-output causal paths determined in step (i) and extension of their causal implications

(iii) Causal completion of the bond graph using classical causality assignment procedures such as SCAP [**10**].

3.2. Bond graph interpretation of essential orders.

Various systems structural properties presented through matrix computation in the previous section can be derived from a graphical approach using bond graph causality.

Property 3 [**23**]

On a forward bond graph model, the essential order of the *i*-th output y_i is given by

$$\overline{\alpha}_{\mathrm{R}i} = L_m - \sum_{\substack{j=1 \\ j\neq i}}^{m} l_{y_j} \; ; \quad i = 1,2,\cdots,m \tag{22}$$

where L_m is the sum of the lengths of m shortest disjoint input-output causal paths

and l_{y_j} is the length of the shortest causal path linking any input component to the output y_i.

(l_{y_j} is also known as the relative degree of the *j*-th output y_i).

Definition 6 [**23**]

In the inverse bond graph model, the order $\omega(p)$ of an output-input causal path p is defined as $\omega(p) = n_D(p) - n_I(p)$, where $n_I(p)$ (resp. $n_D(p)$) is the number of energy storage elements in integral (resp. derivative) causality met when following the path p. This number determines the net number of derivation between the output and the input.

Remark 3

The length and order of causal paths, as given in Definition 5 and 6 above in the context of forward and inverse bond graph models respectively, are opposite of each other and defined so that these numbers are non negative for physical systems modelled by bond graph. These numbers refer to natural input-output integrations in forward models and the associated output-input derivations in inverse models.

From the Definition 6 above and the remark that the essential order $\bar{\alpha}_{\mathrm{R}i}$ of the *i*-th output is the highest derivative of the *i*-th output appearing in the inverse model (Property 2), a property equivalent to Property 3 can be stated as follow.

Property 4 [**23**]

On the inverse bond graph model, the essential order of the *i*-th output y_i is the highest order of the causal path linking the output y_i to any input component.

Dual version of the above properties related to the essential orders of the inputs can now be stated.

Property 5

On a bond graph model, the essential order of the *i*-th input u_i is given by

$$\bar{\alpha}_{\mathrm{L}i} = L_m - \sum_{\substack{j=1 \\ j\neq i}}^{m} l_{u_j} \; ; \quad i = 1,2,\cdots,m \tag{23}$$

where L_m is the sum of the lengths of m shortest disjoint input-output causal paths.

and l_{u_j} is the length of the shortest causal path linking the *j*-th input u_j to any output component.

Property 6

On the inverse bond graph model, the essential order of the *i*-th input u_i is the highest order of the causal path linking any output component to the input u_i.

3.3 Bond graph based configuration for filtered inversion

Mathematical models derived from inverse bond graphs obtained from the procedure in section 3.1 are non-proper as they require differentiators. An alternative to the exact inversion is to consider an approximate or filtered inverse by cascading the inverse model with an appropriate pre- or post-filter (or another physical system) with appropriate structural dynamic properties so that the overall system is a proper dynamical system. In particular for right filtered inverse, the relative degrees $\rho_{\mathrm{R}i}$ of the filters should be at least equal to the essential orders $\overline{\alpha}_{\mathrm{R}i}$ of the outputs[2] and for left filtered inverse the relative degrees $\rho_{\mathrm{L}i}$ of the filters should at least equal to the essential order $\overline{\alpha}_{\mathrm{L}i}$ of the inputs:

$$\rho_{\mathrm{R}i} \geq \overline{\alpha}_{\mathrm{R}i};\ i = 1,2,\cdots,m \tag{24}$$

$$\rho_{\mathrm{L}i} \geq \overline{\alpha}_{\mathrm{L}i};\ i = 1,2,\cdots,m \tag{25}$$

In the above structural conditions (24) and (25), the case where the filters are chosen so that the relative degrees are equal to the essential orders will lead to filtered inverses that are proper with direct transmission terms that will carry through the measurement or specification noise. To avoid this, the filters relative degrees should be strictly greater than the essential orders so that the filtered inverses are strictly proper.

Generalising the physical specification based inversion presented in [**15**] for single-input single-output systems, bond graph based configurations for filtered inversion are given in Fig. 1 and Fig. 2 for right and left filtered inverse models respectively. In order to represent various possible configurations associated with the type of input and output variables (effort or flow), the input u_1 and the output y_1 of the actual system are assumed to be effort variables while the input u_n and the output y_n of the actual system are assumed to be flow variables.

For the right filtered inverse configuration (Fig.1), **SS** : *zero* elements perform the isolation of the filtered desired outputs $y_{\mathrm{F}i}$ which act as input to the inverse of the actual system to compute the filtered or required inputs $u_{\mathrm{F}i}$. This is done by connecting the **SS** : *zero* element to a 1 or 0 junction if the output is an effort of a flow variable respectively. As for the left filtered inverse configuration (Fig. 2), the isolation of the output of the exact inverse model for post-filtering is done using a unit effort amplifier **AE** or a unit flow amplifier **AF** depending whether the input is an effort or a flow variable respectively.

[2] In the context of specification based (or right filtered) inversion in [**15**], the structural condition that the relative degree of the right filter should be greater than the relative degree of the system is true for monovariable systems but not necessarily for multivariable systems.

As a reminder, the **SS**-element is a non-standard bond graph element that generalises and replaces sources and sensors elements to enable flexible causality assignments associated with various computational problems. Non-standard **AE** and **AF** elements are two-port interpretation of active bonds associated with effort and flow variables. Their constitutive equations ensure that the power flow is zero and the introduction of these elements by Gawthrop [**11**,**13**] proved to be very convenient in the context of bicausal bond graphs. Details on these elements are also given in [**15**].

Remark 4

Because the right inverse is used to determine an input required to achieve a desired output for the actual system, in Fig. 1, the Filter_R*i* can also be referred to as Specification Systems and the inverse problem under consideration will then be that of determining the inputs to the actual system so that its outputs behave like the outputs of the Specification Systems subject to the inputs u_{si} [**15**].

3.4 Mathematical models from bond graph based right filtered inverse

Mathematical equations derived from the bond graph configurations in Fig. 1 and Fig. 2 are not readily available in the form of standard state space equations (1) and require some symbolic manipulations to be rewritten in this form. The right filtered inverse model derived from the composite bond graph in Fig.1 can in the first instance be written as

$$\begin{cases} \dot{\bar{\boldsymbol{x}}} = \bar{\mathbf{A}}\,\bar{\boldsymbol{x}} + \sum_{i=1}^{m}\sum_{k=0}^{\bar{\alpha}_{\mathrm{R}i}} \bar{\boldsymbol{b}}_{ik}\, y_{\mathrm{F}i}{}^{(\boldsymbol{k})} \\ \boldsymbol{u}_{\mathrm{F}} = \bar{\mathbf{C}}\,\bar{\boldsymbol{x}} + \sum_{i=1}^{m}\sum_{k=0}^{\bar{\alpha}_{\mathrm{R}i}} \bar{\boldsymbol{d}}_{ik}\, y_{\mathrm{F}i}{}^{(\boldsymbol{k})} \end{cases} \tag{26a}$$

$$\begin{cases} \dot{\boldsymbol{x}}_{\mathrm{R}i} = \mathbf{A}_{\mathrm{R}i}\boldsymbol{x}_{\mathrm{R}i} + \boldsymbol{b}_{\mathrm{R}i}\, y_i \\ y_{\mathrm{F}i} = \mathbf{C}_{\mathrm{R}i}\boldsymbol{x}_{\mathrm{R}i} \end{cases} ; i = 1,2,\cdots,m \tag{26b}$$

Equations (26a) represent the inverse model of the actual system where $\boldsymbol{u}_{\mathrm{F}}$ is the vector of filtered inputs to be calculated, $\bar{\boldsymbol{x}}$ is the minimal-order state vector (associated with energy storage elements that remain in integral causality in the inverse bond graph), $y_{\mathrm{F}i}{}^{(\boldsymbol{k})}$ are the derivatives of the outputs from the chosen filters (or specification systems), matrices $\bar{\mathbf{A}}$, $\bar{\mathbf{C}}$ and vectors $\bar{\boldsymbol{b}}_{ik}$, $\bar{\boldsymbol{d}}_{ik}$ are of appropriate dimensions and obtained from the inverse bond graph model. Equations (26b) represent the state-space model of the so-called Filter_R*i;*

$i = 1,2,\cdots,m$ with $\boldsymbol{x}_{\mathrm{R}i}$ the state vectors, matrices $\mathbf{A}_{\mathrm{R}i}$, $\mathbf{C}_{\mathrm{R}i}$ and vector $\boldsymbol{b}_{\mathrm{R}i}$ are of appropriate dimensions and derived from the bond graph model of each Filter_R*i*. Equations (26a) are conveniently written so that the derivatives of the outputs from the filters $y_{\mathrm{F}i}^{(\boldsymbol{k})}$ appear explicitly.

To rearrange the set of equations (26a) and (26b) into the standard state space representation, if the filters are chosen so that the structural condition (24) i.e. $\rho_{\mathrm{R}i} \geq \overline{\alpha}_{\mathrm{R}i}$; $i = 1,2,\cdots,m$ are satisfied, then all the successive derivatives $y_{\mathrm{F}i}^{(\boldsymbol{k})}$; $k = 1,2,\cdots,\overline{\alpha}_{\mathrm{R}i}$ can be obtained from (26b) as functions of the state variables $\boldsymbol{x}_{\mathrm{R}i}$ and eventually the input y_i and substituted into (26a). The state equation of the right filtered inverse may then be written as

$$\begin{cases} \dot{\boldsymbol{x}}_{\mathrm{R}1} = \mathbf{A}_{\mathrm{R}1}\boldsymbol{x}_{\mathrm{R}1} + \boldsymbol{b}_{\mathrm{R}1}y_1 \\ \vdots \\ \dot{\boldsymbol{x}}_{\mathrm{R}m} = \mathbf{A}_{\mathrm{R}m}\boldsymbol{x}_{\mathrm{R}m} + \boldsymbol{b}_{\mathrm{R}m}y_m \\ \dot{\overline{\boldsymbol{x}}} = \overline{\mathbf{A}}\,\overline{\boldsymbol{x}} + \sum_{i=1}^{m}\sum_{k=1}^{\overline{\alpha}_{\mathrm{R}i}} \overline{\boldsymbol{b}}_{ik}\mathbf{C}_{\mathrm{R}i}\mathbf{A}_{\mathrm{R}i}^{k}\boldsymbol{x}_{\mathrm{R}i} + \sum_{i=1}^{m} \overline{\boldsymbol{b}}_{i\rho_{Ri}}\mathbf{C}_{\mathrm{R}i}\mathbf{A}_{\mathrm{R}i}^{\rho_{Ri}-1}\boldsymbol{b}_{\mathrm{R}\rho_{Ri}}y_i \\ \boldsymbol{u}_{\mathrm{F}} = \overline{\mathbf{C}}\,\overline{\boldsymbol{x}} + \sum_{i=1}^{m}\sum_{k=1}^{\overline{\alpha}_{\mathrm{R}i}} \overline{\boldsymbol{d}}_{ik}\mathbf{C}_{\mathrm{R}i}\mathbf{A}_{\mathrm{R}i}^{k}\boldsymbol{x}_{\mathrm{R}i} + \sum_{i=1}^{m} \overline{\boldsymbol{d}}_{i\rho_{Ri}}\mathbf{C}_{\mathrm{R}i}\mathbf{A}_{\mathrm{R}i}^{\rho_{Ri}-1}\boldsymbol{b}_{\mathrm{R}\rho_{Ri}}y_i \end{cases} \tag{27}$$

In (27), the last summation terms $\sum_{i=1}^{m} \overline{\boldsymbol{b}}_{i\rho_{Ri}}\mathbf{C}_{\mathrm{R}i}\mathbf{A}_{\mathrm{R}i}^{\rho_{Ri}-1}\boldsymbol{b}_{\mathrm{R}\rho_{Ri}}y_i$ in the expression of $\dot{\overline{\boldsymbol{x}}}$ and the direct transmission term $\sum_{i=1}^{m} \overline{\boldsymbol{d}}_{i\rho_{Ri}}\mathbf{C}_{\mathrm{R}i}\mathbf{A}_{\mathrm{R}i}^{\rho_{Ri}-1}\boldsymbol{b}_{\mathrm{R}\rho_{Ri}}y_i$ in the expression of $\boldsymbol{u}_{\mathrm{F}}$ are present only in the case where $\rho_{\mathrm{R}i} = \overline{\alpha}_{\mathrm{R}i}$.

3.5 Mathematical models from bond graph based left filtered inverse

For the left filtered inverse model in Fig. 2, the equations that are derived from the composite bond graph model can be written in the first instance as

$$\begin{cases} \dot{\overline{\boldsymbol{x}}} = \overline{\mathbf{A}}\,\overline{\boldsymbol{x}} + \sum_{k=0}^{\overline{\alpha}_{\mathrm{L}}} \overline{\mathbf{B}}_k\,\boldsymbol{y}^{(\boldsymbol{k})} \\ u_i = \overline{\boldsymbol{c}}_{\boldsymbol{i}}\,\overline{\boldsymbol{x}} + \sum_{k=0}^{\overline{\alpha}_{\mathrm{L}i}} \overline{\boldsymbol{d}}_{ki}\,\boldsymbol{y}^{(\boldsymbol{k})}\,; \quad i = 1,2,\cdots,m \end{cases} \tag{28a}$$

$$\begin{cases} \dot{\boldsymbol{x}}_{\mathrm{L}i} = \mathbf{A}_{\mathrm{L}i}\boldsymbol{x}_{\mathrm{L}i} + \boldsymbol{b}_{\mathrm{L}i}u_i \\ u_{\mathrm{F}i} = \boldsymbol{c}_{\mathrm{L}i}\boldsymbol{x}_{\mathrm{L}i} \end{cases};\ i = 1,2,\cdots,m \tag{28b}$$

Equations (28a) represent the inverse model of the actual system written for convenience in a different form to that of equations (26a). In this case, individual inputs u_i are expressed explicitly. Equations (28b) represent the state-space model of the Filter_Li; $i = 1,2,\cdots,m$. Substituting the expression of u_i from (28a) into the first line of (28b) and combining the state vector of the inverse system and that of the filters leads to the mathematical model that can be written as

$$\begin{cases} \dot{\xi} = \widetilde{\mathbf{A}}\,\xi + \sum_{k=0}^{\overline{\alpha}_{\mathrm{L}}} \widetilde{\mathbf{B}}_k \boldsymbol{y}^{(k)} \\ \boldsymbol{u}_{\mathrm{F}} = \widetilde{\mathbf{C}}\,\xi \end{cases} \tag{29}$$

where the block partitioned vectors and matrices are

$$\xi = \begin{pmatrix} \overline{\boldsymbol{x}} \\ \dot{\boldsymbol{x}}_{\mathrm{L}1} \\ \vdots \\ \dot{\boldsymbol{x}}_{\mathrm{L}m} \end{pmatrix};\ \widetilde{\mathbf{A}} = \begin{bmatrix} \overline{\mathbf{A}} & \mathbf{0} & \mathbf{0} & \cdots & \mathbf{0} \\ \boldsymbol{b}_{\mathrm{L}1}\bar{\boldsymbol{c}}_1 & \mathbf{A}_{\mathrm{L}1} & \mathbf{0} & \cdots & \mathbf{0} \\ & \mathbf{0} & \ddots & \cdots & \vdots \\ \vdots & \vdots & \vdots & \ddots & \mathbf{0} \\ \boldsymbol{b}_{\mathrm{L}m}\bar{\boldsymbol{c}}_m & \mathbf{0} & \mathbf{0} & \cdots & \mathbf{A}_{\mathrm{L}m} \end{bmatrix};\ \widetilde{\mathbf{B}}_{\mathrm{k}} = \begin{pmatrix} \overline{\mathbf{B}}_{\mathrm{k}} \\ \boldsymbol{b}_{\mathrm{L}1}\bar{\boldsymbol{d}}_{\mathrm{k}1} \\ \vdots \\ \boldsymbol{b}_{\mathrm{L}m}\bar{\boldsymbol{d}}_{km} \end{pmatrix} \text{ and } \widetilde{\mathbf{C}} = \begin{bmatrix} \mathbf{0} & \boldsymbol{c}_{\mathrm{L}1} & \mathbf{0} & \cdots & \mathbf{0} \\ \mathbf{0} & \mathbf{0} & \boldsymbol{c}_{\mathrm{L}2} & & \vdots \\ \vdots & \vdots & & \ddots & \mathbf{0} \\ \mathbf{0} & \mathbf{0} & & \cdots & \boldsymbol{c}_{\mathrm{L}m} \end{bmatrix} \tag{30}$$

Equation (29) still contains the derivatives of the inverse model inputs ($\boldsymbol{y}^{(k)}$ in this case) despite the overall model being *a priori* a proper dynamic system if the structural condition (25) is met. From the configuration in Fig.2, this situation arises from the structure of the system where the derivatives $\boldsymbol{y}^{(k)}$ from the exact inverse model are integrated in a latter stage through the left filters Filter-L*i*s. To transform (29) into a state space equation model that does not contain any time derivative of the inputs, the following lemma is proposed which is a generalisation of the procedure for the elimination of time derivatives of inputs presented in [**24**] in the case of forward model containing a first order derivative of the input.

Lemma 1

Consider a system with input $\boldsymbol{y}(t)$ and output $\boldsymbol{u}(t)$ described by the equations

$$\begin{cases} \dot{\boldsymbol{x}}(t) = \mathbf{A}\boldsymbol{x}(t) + \sum_{k=0}^{p} \mathbf{B}_k \boldsymbol{y}^{(k)}(t) \\ \boldsymbol{u}(t) = \mathbf{C}\boldsymbol{x}(t) \end{cases} \tag{31}$$

where the output matrix $\mathbf{C}$ is so that $\sum_{j=1}^{p-i} \mathbf{C}\mathbf{A}^{j-1}\mathbf{B}_{j+i} = \mathbf{0}$ for $i = 1,2,\cdots,p-1$ (32)

The state transformation $\boldsymbol{z}(t) = \boldsymbol{x}(t) - \sum_{i=0}^{p-1}\sum_{j=1}^{p-i} \mathbf{A}^{j-1}\mathbf{B}_{j+i}\boldsymbol{y}^{(i)}(t)$ (33)

leads to the following dynamical state equation form that does not contain any time derivative of the inputs

$$\begin{cases} \dot{\boldsymbol{z}}(t) = \mathbf{A}\boldsymbol{z}(t) + \sum_{k=0}^{p} \mathbf{A}^{k}\mathbf{B}_{k}\boldsymbol{y}(t) \\ \boldsymbol{u}(t) = \mathbf{C}\boldsymbol{z}(t) + \sum_{j=1}^{p} \mathbf{C}\mathbf{A}^{j-1}\mathbf{B}_{j}\boldsymbol{y}(t) \end{cases} \tag{34}$$

The proof of this lemma is given in the Appendix A.

If the left filters Filter-Li are chosen so that the structural conditions (25) i.e. $\rho_{\mathrm{L}i} \geq \overline{\alpha}_{\mathrm{L}i}$; $i = 1,2,\cdots,m$ are satisfied, then from (28b), $\boldsymbol{c}_{\mathrm{L}i}\mathbf{A}_{\mathrm{L}i}^{j-1}\boldsymbol{b}_{\mathrm{L}i} = \mathbf{0}$ for $j = 1,\cdots,\overline{\alpha}_{\mathrm{L}i}$ and for this reason, it can easily be verified the matrices $\tilde{\mathbf{A}}$, $\tilde{\mathbf{B}}_{k}$ and $\tilde{\mathbf{C}}$ in (30) associated with the equation (29) are so that $\sum_{j=1}^{\overline{\alpha}_{\mathrm{L}}-i} \tilde{\mathbf{C}}\tilde{\mathbf{A}}^{j-1}\tilde{\mathbf{B}}_{j+i} = \mathbf{0}$ for $i = 1,2,\cdots,\overline{\alpha}_{\mathrm{L}i} - 1$ (i.e. condition (32) in Lemma 1 is satisfy).

Therefore, applying the state transformation (33)

$$\boldsymbol{z}(t) = \xi(t) - \sum_{i=0}^{\overline{\alpha}_{\mathrm{L}}-1}\sum_{j=1}^{\overline{\alpha}_{\mathrm{L}}-i} \tilde{\mathbf{A}}^{j-1}\tilde{\mathbf{B}}_{j+i}\boldsymbol{y}^{(i)}(t) \tag{35}$$

to the left filtered inverse model (29) leads to the standard state equation without the need for input differentiators

$$\begin{cases} \dot{\boldsymbol{z}}(t) = \tilde{\mathbf{A}}\boldsymbol{z}(t) + \sum_{k=0}^{\overline{\alpha}_{\mathrm{L}}} \tilde{\mathbf{A}}^{k}\tilde{\mathbf{B}}_{k}\boldsymbol{y}(t) \\ \boldsymbol{u}_{\mathrm{F}}(t) = \tilde{\mathbf{C}}\boldsymbol{z}(t) + \sum_{j=1}^{\overline{\alpha}_{\mathrm{L}}} \tilde{\mathbf{C}}\tilde{\mathbf{A}}^{j-1}\tilde{\mathbf{B}}_{j}\boldsymbol{y}(t) \end{cases} \tag{36}$$

4. EXAMPLE

In this section, an illustrative example is presented for a two-input two-output linear system. Consider the electrical circuit given in Fig. 3 where the inputs are the voltage source u_1 and the current source u_2 and the

outputs are chosen as the voltage y_1 across the capacitor C_1 and the current y_2 through the inductor L_2. The (forward) bond graph model of the system is shown in Fig. 4 and the inverse bond graph obtained from applying the procedure proposed in [**14**] is given in Fig. 5. The minimal-order inverse model directly derived from the inverse bond graph in Fig. 5 is given by (37) where the unique state variable q_2 is the energy variable (charge) of the capacitor C_2. Because of the differentiators required for the realisation of this model, its numerical implementation is not easy and both the right and left filtered inverse models which are approximate but proper will be considered in the sequel.

$$\begin{cases} \dot{q}_2 = -\frac{1}{RC_2} q_2 + \frac{L_2}{R} \dot{y}_2 \\ u_1 = \frac{L_1}{R^2 C_2^2} q_2 + L_1 C_2 \ddot{y}_1 + \frac{L_1 L_2}{R} \ddot{y}_2 - \frac{L_1 L_2}{R^2 C_2} \dot{y}_2 + L_1 \dot{y}_2 + y_1 \\ u_2 = -\frac{1}{C_2^2} q_2 + \frac{L_2}{R} \dot{y}_2 + y_2 \end{cases} \tag{37}$$

4.1 Right filtered inverse

From the forward bond graph model in Fig. 4, it can easily be seen that the sum of the lengths of the 2 shortest disjoint input-output causal paths is $L_2 = 3$ (length 2 between u_1 and y_1 and length 1 between u_2 and y_2). However the length of the shortest causal path linking any input component to the outputs (or relative degrees) as defined in Property 3 are respectively $l_{y_1} = 1$ (between u_2 and y_1 via C_1) and $l_{y_2} = 1$ (between u_2 and y_2 as indicated in Fig.4). It can therefore be deduced that the essential orders of the outputs as defined in (22) are respectively $\overline{\alpha}_{R1} = 2$ and $\overline{\alpha}_{R2} = 2$. This result can also be derived from the inverse bond graph in Fig. 5 using Property 4 where the highest order of the causal path linking the outputs to any input component can be verified to be respectively $\overline{\alpha}_{R1} = 2$ and $\overline{\alpha}_{R2} = 2$. In the reduced inverse model (37), it can also be seen that the highest derivation order of the output y_1 is 2 and that of y_2 is also 2 which coincide with the outputs essential orders $\overline{\alpha}_{R1}$ and $\overline{\alpha}_{R2}$ (Property 2).

Therefore, the relative degrees of the right filters Filter_R1 and Filter_R2 (or any performance specification systems on the outputs y_1 and y_2) in Fig. 1 should be at least 2 for each output if the overall filtered inverse system dynamic is to be proper.

In this example, the right filters Filter_R*i* or specification systems are chosen as RLC circuits in serial or parallel configurations and driven by voltage or current sources with the output selected so as to match the effort or flow variable type of the output and to satisfy the relative degree conditions (23). The overall right filtered inverse configuration is given in Fig. 6.

For the purpose of the illustration, if all physical parameters (of the actual system and the filters) are set equal to one, the equations of the right filtered inverse model derived from the bond graph configuration in Fig. 6 can be written, after symbolic manipulations to perform the substitution of the derivatives of the outputs, as follows

$$\begin{cases} \dot{\boldsymbol{x}} = \begin{bmatrix} -1 & -1 & 0 & 0 & 0 \\ 1 & 0 & 0 & 0 & 0 \\ 0 & 0 & -1 & -1 & 0 \\ 0 & 0 & 1 & 0 & 0 \\ 0 & 0 & 1 & 0 & -1 \end{bmatrix} \boldsymbol{x} + \begin{bmatrix} 1 & 0 \\ 0 & 0 \\ 0 & 1 \\ 0 & 0 \\ 0 & 0 \end{bmatrix} \boldsymbol{y} \\ \boldsymbol{u}_{\mathrm{F}} = \begin{bmatrix} -1 & 0 & -1 & -1 & 1 \\ 0 & 0 & 1 & 1 & -1 \end{bmatrix} \boldsymbol{x} + \begin{bmatrix} 1 & 1 \\ 0 & 0 \end{bmatrix} \boldsymbol{y} \end{cases} \tag{38}$$

with $\boldsymbol{x}^{\mathrm{T}} = [p_{\mathrm{s1}} \;\; q_{\mathrm{s1}} \;\; q_{\mathrm{s2}} \;\; p_{\mathrm{s2}} \;\; q_2]^{\mathrm{T}}$ associated with the energy variables indicated in Fig. 6; $\boldsymbol{y}^{\mathrm{T}} = [y_1 \;\; y_2]^{\mathrm{T}}$ and $\boldsymbol{u}_{\mathrm{F}}^{\mathrm{T}} = [u_{\mathrm{F1}} \;\; u_{\mathrm{F2}}]^{\mathrm{T}}$

This system is proper and can be numerically implemented without difficulty. If for instance the inputs to the Filter_R*i* or specification systems y_1 and y_2 are set as unit step inputs, the right inverse problem considered is therefore that of computing the inputs u_{F1} and u_{F2} so that the outputs of the actual system in Fig. 3 behave like the outputs of the RLC specification systems subject to unit step inputs. With all parameters set to one and unit step inputs y_2 starting at $t = 1\,\mathrm{s}$ and y_1 starting at $t = 10\,\mathrm{s}$, the simulation results are shown in Fig. 7 and 8. Fig. 7 shows the step input y_2 to the specification system 2 and the output of this system y_{F2} which is the desired output of the actual system (the input y_1 and the desired output y_{F1} are identical to y_2 and y_{F2} but starting at $t = 10\,\mathrm{s}$). Fig. 8 shows the computed inputs u_{F1} and u_{F2} to achieve the outputs y_{F1} and y_{F2}.

4.2 Left filtered inverse

As previously noticed, the sum of the lengths of the 2 shortest disjoint input-output causal paths is $L_2 = 3$ and it can now be seen from the forward bond graph model in Fig. 4 that the length of the shortest causal path linking

the input to any output component are respectively $l_{u_1} = 2$ and $l_{u_2} = 1$. Therefore the essential orders of the inputs as defined in (23) are respectively $\bar{\alpha}_{\mathrm{L}1} = 2$ and $\bar{\alpha}_{\mathrm{L}2} = 1$.

This result can also be derived from the inverse bond using Property 6 where the highest order of the causal path linking any output component to the inputs $u_1(t)$ and $u_2(t)$ can be verified to be respectively $\bar{\alpha}_{\mathrm{L}1} = 2$ and $\bar{\alpha}_{\mathrm{L}2} = 1$. It can also be seen from the inverse model equation (37) that input essential orders coincide with the highest derivative of the output components appearing in the *i*-th input component $u_i(t)$ (Property 1).

In this case, to satisfy the structural conditions (25), the left filters chosen are a RLC circuit with a relative order $\rho_{\mathrm{L}1} = 2$ for the input $u_1(t)$ and a RL circuit with a relative order $\rho_{\mathrm{L}2} = 1$ for the input $u_2(t)$. The overall left filtered inverse configuration is given in Fig. 9.

For the purpose of the illustration, all physical parameters for the actual system and for the filters are again set equal to one. The equations of the left filtered inverse derived from the bond graph configuration in Fig. 8 can be written after some simple symbolic manipulations as follows

$$\begin{cases} \dot{\boldsymbol{x}} = \mathbf{A}\boldsymbol{x} + \mathbf{B}_0\boldsymbol{y} + \mathbf{B}_1\dot{\boldsymbol{y}} + \mathbf{B}_2\ddot{\boldsymbol{y}} \\ \boldsymbol{u}_{\mathrm{F}} = \mathbf{C}\boldsymbol{x} \end{cases} \tag{39}$$

with $\boldsymbol{x}^{\mathrm{T}} = [\, q_2 \quad p_{\mathrm{F}1} \quad q_{\mathrm{F}1} \quad p_{\mathrm{F}2} \,]^{\mathrm{T}}$ associated with the energy variables indicated in Fig. 9; $\boldsymbol{y}^{\mathrm{T}} = [y_1 \;\; y_2]^{\mathrm{T}}$ and $\boldsymbol{u}_{\mathrm{F}}^{\mathrm{T}} = [u_{\mathrm{F}1} \;\; u_{\mathrm{F}2}]^{\mathrm{T}}$

and $\mathbf{A} = \begin{bmatrix} -1 & 0 & 0 & 0 \\ 1 & -1 & -1 & 0 \\ 0 & 1 & 0 & 0 \\ -1 & 0 & 0 & -1 \end{bmatrix}$; $\mathbf{B}_0 = \begin{bmatrix} 0 & 0 \\ 1 & 0 \\ 0 & 0 \\ 0 & 1 \end{bmatrix}$; $\mathbf{B}_1 = \begin{bmatrix} 0 & 1 \\ 0 & 0 \\ 0 & 0 \\ 0 & 1 \end{bmatrix}$; $\mathbf{B}_2 = \begin{bmatrix} 0 & 0 \\ 1 & 1 \\ 0 & 0 \\ 0 & 0 \end{bmatrix}$; $\mathbf{C} = \begin{bmatrix} 0 & 0 & 1 & 0 \\ 0 & 0 & 0 & 1 \end{bmatrix}$

Equation (39) contains the derivatives of the inputs to the inverse system and this can cause problems in their numerical implementation. To overcome this issue, the state vector transformation $\boldsymbol{z} = \boldsymbol{x} - \left(\mathbf{B}_1 + \mathbf{A}\mathbf{B}_2\right)\boldsymbol{y} - \mathbf{B}_2\dot{\boldsymbol{y}}$ according to (33) in Lemma 1 is performed on the model (39) and leads to the state equations in the standard form of a proper dynamical system

$$\begin{cases} \dot{\boldsymbol{z}} = \mathbf{A}\boldsymbol{z} + \left(\mathbf{B}_0 + \mathbf{A}\mathbf{B}_1 + \mathbf{A}^2\mathbf{B}_2\right)\boldsymbol{y} \\ \boldsymbol{u}_{\mathrm{F}} = \mathbf{C}\boldsymbol{z} + \left(\mathbf{C}\mathbf{B}_1 + \mathbf{C}\mathbf{A}\mathbf{B}_2\right)\boldsymbol{y} \end{cases} \tag{40a}$$

$$\begin{cases} \dot{\boldsymbol{z}} = \begin{bmatrix} -1 & 0 & 0 & 0 \\ 1 & -1 & -1 & 0 \\ 0 & 1 & 0 & 0 \\ -1 & 0 & 0 & -1 \end{bmatrix} \boldsymbol{z} + \begin{bmatrix} 0 & -1 \\ 1 & 1 \\ -1 & -1 \\ 0 & -1 \end{bmatrix} \boldsymbol{y} \\ \boldsymbol{u}_{\mathrm{F}} = \begin{bmatrix} 0 & 0 & 1 & 0 \\ 0 & 0 & 0 & 1 \end{bmatrix} \boldsymbol{z} + \begin{bmatrix} 1 & 1 \\ 0 & 1 \end{bmatrix} \boldsymbol{y} \end{cases} \tag{40b}$$

Now assume that the computed inputs u_{F1} and u_{F2} from the right filtered inverse (Fig. 8) are applied to the actual system in Fig.3 and consider the problem of reconstructing these inputs from the measurement of the outputs y_1 and y_2 of the actual system. To emphasize the merit of the filtered inverse, the exact inverse model (37) with derivative blocks was first cascaded with the actual system and implemented in the Simulink® environment. While it was possible to reconstruct the input u_{F2} (Fig.10b) in this manner, numerical instabilities prevented the reconstruction of u_{F1} (Fig.10a). It is certain that adding any measurement noise to the output of the actual system will increase the numerical instability problem and make it more difficult to reconstruct any of the outputs including u_{F2}.

The above left filtered inverse model (40b), with all filters parameters set to one, was then cascaded with the actual system and the reconstructed inputs are shown in Fig. 11. Although there are no numerical issues with this simulation, the reconstruction of the input u_1 is relatively inaccurate (Fig.11a) while there is a noticeable phase lag for the input u_2 (Fig.11b). These results are due to the choice of the parameters of the filters that imposes a too low band pass to the left filtered inverse model. To improve the accuracy of the inputs reconstruction, a different set of parameters was chosen for the filters as indicated in Table 1, referring to bond graph model in Fig.9

$C_{\mathrm{F1}} = 0.001\,\mathrm{F}$	$L_{\mathrm{F1}} = 0.1\,\mathrm{H}$	$R_{\mathrm{F1}} = 100\,\Omega$	$L_{\mathrm{F2}} = 0.001\,\mathrm{H}$	$R_{\mathrm{F2}} = 1\,\Omega$

Table 1. Alternative set of parameters for the filters of the left filtered inverse model in Fig.9

With the set of parameters in Table 1, the simulation results are presented in Fig.12 indicating that the left filtered inverse model in this case reconstructs the inputs relatively well.

5. DISCUSSION

The filtered inversion technique presented in this paper enables to formally obtain an approximate right or left inverse model that is dynamical and does not require differentiators for its realisation. As demonstrated in the

example in section 4, there are two separate issues that are to be considered: (i) the structural properties of the filters in terms of their relative degrees compared to the essential orders as given by (24) & (25) and (ii) the choice of numerical parameters for the filters that will depend on the model inputs.

Although the method presented can be applied independently of the bond graph representation, it is clear that this modelling tool provides a convenient framework for the structural analysis and also lends itself to the extension of the methodology to nonlinear systems. In section 2, classical approach to system inversion and filtered inversion are presented for linear systems using state space and transfer function representation. However, the bond graph interpretation of the associated concepts in section 3.1 to 3.3 does not necessarily assume the linearity of the bond graph model.

Even if the system is nonlinear, right filtered inversion or specification-based inversion as it was called in [**15**] can still be applied using bond graph representation. In this case, the Filter_R*i*s or specification systems in Fig. 1 will be the bond graph models of given linear or nonlinear systems that meet the structural property (24) and prescribe the desired performance of the actual system. Mathematical models symbolic manipulations from (26) to (27) presented for the linear case can also be performed, if allowed by the type of nonlinearities, to eliminate the derivatives of the outputs in the final state space model. Also, the choice of the numerical parameters for the specification system in the right inversion is less constrained as it is dictated by the desired output performance of the actual system for which the designer would like to determine the associated input.

For left filtered inverse, given that the problem is to reconstruct the inputs from the measured outputs, the choice of the numerical parameters for the Filter_L*i*s is very important for good approximation of the inputs. These have to take into consideration not only the assumed frequency spectrum of the system inputs but also the noise level that may affect the measurement. If the actual system is nonlinear, the symbolic manipulations to get the mathematical model in the form similar to (29) with the derivatives of the outputs are feasible. However, the kind of state transformation proposed in Lemma 1 to eliminate the derivatives of the outputs is not obvious in the nonlinear case. Although, a procedure to eliminate a first order derivative of the input from a nonlinear mathematical model with a certain format is proposed in [**24**], the extension to higher order derivatives of the inputs as it would be the case with inverse models could be the topic for further research.

6. CONCLUSIONS

A problem associated with exact inverse models is that they generally require differentiators for their realisation leading to numerical implementations that are usually computationally inefficient. To address this issue for

physical systems, bond graph based filtered inverse models are proposed in this paper as a method to derive approximate inverse that are proper dynamical models. Using bond graph representation, it has been shown that some structural analysis can be performed on the original system to determine the properties of the filters to be cascaded with the original system to obtain approximate inverses that are proper. Bond graph based configurations to represent filtered inverse models that enable the automated generation of inverse model equations are proposed. It is however noted that the equations generated require some symbolic manipulations and some state transformation in the case of left filtered inverse in order to get the standard state space model without the derivatives of the inputs. The extension of the proposed methodology to nonlinear systems is discussed and while there are no major issues with the right filtered inversion, further work needs to be done for left filtered inversion.

REFERENCES

1 **Brockett, R. W.** and **Mesarovic, M.D.** The reproducibility of multivariable systems, *Journal of Mathematical Analysis and Applications*, 1965, **11**, 548 – 563.

2 **Silverman, L. M.** Inversion of multivariable linear systems, *IEEE Trans. Automatic Control*, 1969, **AC-14** (3), 270 – 276.

3 **Sain, M. K.** and **Massey, J. L.** Invertibility of linear time-invariant dynamical systems, *IEEE Trans. Automatic Control*, 1969, **AC-14** (2), 141 – 149.

4 **Seraji, H**. Minimal inversion, command matching and disturbance decoupling in multivariable systems, *Int. Journal of Control*, 1989, **49** (6), 2093 – 2121.

5 **Ye, Y. and Wang, D.** Clean system inversion learning control law, *Automatica*, 2005, **41** (9), 1549 – 1556.

6 **Ngwompo, R. F., Scavarda, S.** and **Thomasset D.** Physical model-based inversion in control systems design using bond graph representation - Part 2: Applications, *Proceedings of the IMechE, Part I: Journal of Systems and Control Engineering*, 2001, **215** (12), 95 – 103.

7 **Thomson, D.** and **Bradley, R.** Inverse simulation as a tool for flight dynamics research - Principles and applications, *Progress in Aerospace Sciences*, 2006, **42** (3), 174 – 210.

8 **Yoshikawa, T.** and **Sugie, T.** Filtered Inverse Systems, *International Journal of Control*, 1986, **43** (6), 1661 – 1671.

9 **Yamada, K., Watanabe, K.** and **Shu, Z. B.** A state space design method of stable filtered inverse systems and its application to H2 suboptimal internal model control, In Proceedings of the 13th Triennial IFAC World Congress, San Francisco, USA, 1996, 379 – 384,.

10 **Karnopp, D. C., Margolis D. L.** and **Rosenberg**, **R.C.** *System Dynamics: A Unified Approach*, 1990 (John Wiley, New York).

11 **Gawthrop, P. J.** and **Smith, L.** *Metamodelling: Bond Graphs and Dynamic Systems*, 1996 (Prentice Hall, Hemel Hempstead).

12 **Gawthrop, P. J.** Bicausal Bond Graphs, In Proceedings of the 1995 Int. Conference on *Bond Graph Modelling and Simulation (ICBGM'95), Simulation Series*, **27** (Eds F.E. Cellier and J.J Granda), Las Vegas, 1995, pp 83-88 (Society for Computer Simulation).

13 **Gawthrop, P. J.** Physical interpretation of inverse dynamics using bicausal bond graphs, *Journal of the Franklin Institute*, 1999, **337**, 743-769.

14 **Ngwompo, R. F., Scavarda, S.** and **Thomasset D.** Physical model-based inversion in control systems design using bond graph representation - Part 1: Theory, *Proceedings of the IMechE, Part I: Journal of Systems and Control Engineering*, 2001, **215** (12), 105 - 112.

15 **Ngwompo, R. F.** and **Gawthrop, P. J.** Bond graph based simulation of nonlinear inverse systems using physical performance specifications, *Journal of the Franklin Institute*, 1999, **336** (8), 1225-1247.

16 **Bonilla, M., Malabre, M.** and **Fonseca, M.** On the approximation of non-proper control laws, *International Journal of Control*, 1997, **68** (4), 775-796.

17 **Pacheco, M. J., Bonilla, M. E.** and **Malabre, M.** Proper exponential approximation of non-proper compensators: the MIMO case, In Proceedings of the 42nd IEEE Conference on Decision and Control, Maui, Hawaii, USA, December 2003, **1**, 110-115.

18 **Kamiyama, S.** and **Furuta, K.** Integral invertibility of linear time invariant systems, *International Journal of Control*, 1977, **25** (3), 403-412.

19 **Commault, C., Descusse, J., Dion, J. M., Lafay, J. F.** and **Malabre, M.** New decoupling invariants: the essential orders, *International Journal of Control*, 1986, **44** (3), 689-700.

20 **Cremer, M.** A precompensator of minimal order for decoupling a linear multivariable systems, *International Journal of Control*, 1971, **14** (6), 1089-1103.

21 Massey, J. L. and **Sain, M. K.** Inverses of linear sequential circuits, *IEEE Trans. on Computers*, 1968, **C-17** (4), 330 – 337.

22 El Feki, M., Di Loreto, M., Bideaux, E., Thomasset, D., and **Ngwompo, R. F.** Structural properties of inverse models represented by bond graph, IFAC Proceedings Volumes (IFAC-PapersOnline), 2008, (**17**) 1.

23 El Feki, M., Di Loreto, M., Bideaux, E., Thomasset, D., and **Marquis-Favre, W.** On the role of essential orders on feedback decoupling and model inversion: bond graph approach, Proceedings 22nd European Conference on Modelling and Simulation, Nicosia, Cyprus, June 2008 (Eds L.S. Louca, Y. Chrysanthou, Z. Oplatkova, K. Al-Begain).

24 Breedveld, P. C. Elimination of time derivatives of sources inputs, In Proceedings of the 2005 Int. Conference on Bond Graph Modelling and Simulation, *Simulation Series*, **37** (1) (Eds F.E. Cellier and J.J Granda), New Orleans, 2005, 39 – 42 (Society for Computer Simulation).

APPENDIX A - Proof of Lemma 1

Consider a system with input $\boldsymbol{y}(t)$ and output $\boldsymbol{u}(t)$ described by the equations

$$\begin{cases} \dot{\boldsymbol{x}}(t) = \mathbf{A}\boldsymbol{x}(t) + \sum_{k=0}^{p} \mathbf{B}_k \boldsymbol{y}^{(k)}(t) \\ \boldsymbol{u}(t) = \mathbf{C}\boldsymbol{x}(t) \end{cases} \tag{A1}$$

With the state transformation $$\boldsymbol{z}(t) = \boldsymbol{x}(t) - \sum_{i=0}^{p-1} \sum_{j=1}^{p-i} \mathbf{A}^{j-1} \mathbf{B}_{j+i} \boldsymbol{y}^{(i)}(t) \tag{A2}$$

Deriving the new state vector $\boldsymbol{z}(t)$ with respect to time and substituting the expression of $\dot{\boldsymbol{x}}(t)$ from (A1) lead to

$$\dot{\boldsymbol{z}}(t) = \mathbf{A}\boldsymbol{x}(t) + \sum_{k=0}^{p} \mathbf{B}_k \boldsymbol{y}^{(k)}(t) - \sum_{i=0}^{p-1} \sum_{j=1}^{p-i} \mathbf{A}^{j-1} \mathbf{B}_{j+i} \boldsymbol{y}^{(i+1)}(t) \tag{A3}$$

The terms with index $j = 1$ in the last double summation cancel the second summation term in (A3) except for the term $\mathbf{B}_0 \boldsymbol{y}(t)$ and therefore (A3) can be simplified into

$$\dot{\boldsymbol{z}}(t) = \mathbf{A}\boldsymbol{x}(t) + \mathbf{B}_0 \boldsymbol{y}(t) - \sum_{i=0}^{p-2} \sum_{j=2}^{p-i} \mathbf{A}^{j-1} \mathbf{B}_{j+i} \boldsymbol{y}^{(i+1)}(t) \tag{A4}$$

Replacing the expression of $\boldsymbol{x}(t)$ obtained from (A2) into (A4) gives

$$\dot{\boldsymbol{z}}(t) = \mathbf{A}\boldsymbol{z}(t) + \mathbf{B}_0 \boldsymbol{y}(t) + \sum_{i=0}^{p-1} \sum_{j=1}^{p-i} \mathbf{A}^{j} \mathbf{B}_{j+i} \boldsymbol{y}^{(i)}(t) - \sum_{i=0}^{p-2} \sum_{j=2}^{p-i} \mathbf{A}^{j-1} \mathbf{B}_{j+i} \boldsymbol{y}^{(i+1)}(t) \tag{A5}$$

This reduces to $$\dot{\boldsymbol{z}}(t) = \mathbf{A}\boldsymbol{z}(t) + \sum_{k=0}^{p} \mathbf{A}^{k}\mathbf{B}_{k}\boldsymbol{y}(t) \tag{A6}$$

Substituting the expression of $\boldsymbol{x}(t)$ obtained from (A2) into the output $\boldsymbol{u}(t) = \mathbf{C}\boldsymbol{x}(t)$ from (A1) gives

$$\boldsymbol{u}(t) = \mathbf{C}\boldsymbol{z}(t) + \sum_{i=0}^{p-1}\sum_{j=1}^{p-i} \mathbf{C}\mathbf{A}^{j-1}\mathbf{B}_{j+i}\boldsymbol{y}^{(i)}(t) \tag{A7}$$

And under the assumption that $\sum_{j=1}^{p-i} \mathbf{C}\mathbf{A}^{j-1}\mathbf{B}_{j+i} = \mathbf{0}$ for $i = 1, 2, \cdots, p-1$, the output can therefore be written as

$$\boldsymbol{u}(t) = \mathbf{C}\boldsymbol{z}(t) + \sum_{j=1}^{p} \mathbf{C}\mathbf{A}^{j-1}\mathbf{B}_{j}\boldsymbol{y}(t) \tag{A8}$$

❑

List of figure captions

Fig. 1 Right filtered inverse bond graph configuration (for the actual system, u_1 and y_1 are assumed to be effort variables while u_n and y_n are assumed to be flow variables). Relative degree $\rho_{\mathrm{R}i}$ of Filter_R*i* should be at least equal to the essential order $\overline{\alpha}_{\mathrm{R}i}$ of the output y_i

Fig. 2 Left filtered inverse bond graph configuration (for the actual system, u_1 and y_1 are assumed to be effort variables while u_n and y_n are assumed to be flow variables). Relative degree $\rho_{\mathrm{L}i}$ of Filter_L*i* should be at least equal to the essential order $\overline{\alpha}_{\mathrm{L}i}$ of the output u_i

Fig. 3 An electrical circuit example

Fig. 4 Forward bond graph model of the electrical circuit in Fig. 3 with minimal length disjoint input-output causal paths indicated

Fig. 5 Inverse bond graph model of the electrical circuit in Fig. 3 with highest order output-input causal paths indicated

Fig. 6 – Right filtered inverse model configuration

Fig. 7 – Right filtered inverse simulation results: step inputs y_1 and y_2 to the Filters or specification systems and resulting prescribed outputs y_{F1} and y_{F2} for the actual system.

Fig. 8 – Right filtered inverse simulation results: computed inputs u_{F1} and u_{F2} to be applied to the actual system in order to achieve the desired filtered outputs y_{F1} and y_{F2} in Fig. 7

Fig. 9 – Left filtered inverse model configuration

Fig. 10 – Response of the exact inverse model cascaded with the actual system to reconstruct the inputs (with all parameters set to one) – (a) Reconstruction of input u_{F1} and (b) Reconstruction of input u_{F2}

Fig. 11 – Response of the left filtered inverse cascaded with the actual system to reconstruct the inputs (with all parameters set to one) – (a) Reconstruction of input u_{F1} and (b) Reconstruction of input u_{F2}

Fig. 12 – Response of the left filtered inverse cascaded with the actual system to reconstruct the inputs (with parameters given in Table 1) – (a) Reconstruction of input u_{F1} and (b) Reconstruction of input u_{F2}

List of Figures

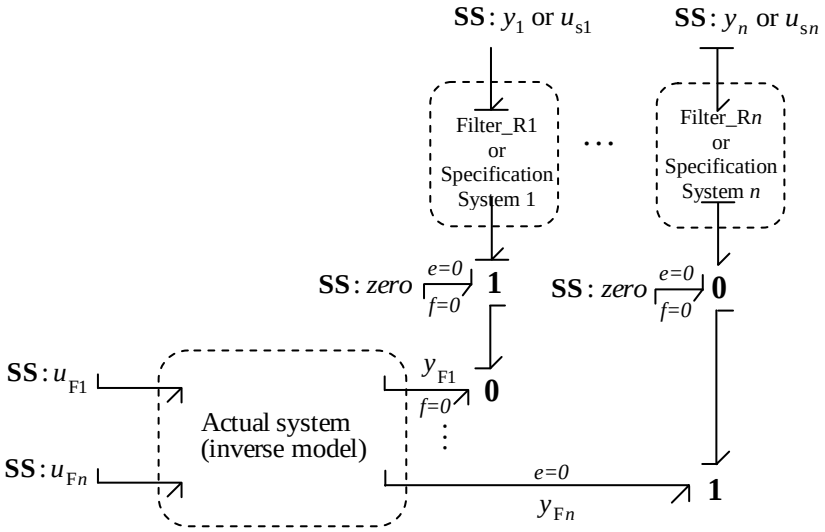

Fig. 1 Right filtered inverse bond graph configuration (for the actual system, u_1 and y_1 are assumed to be effort variables while u_n and y_n are assumed to be flow variables). Relative degree $\rho_{\mathrm{R}i}$ of Filter_R*i* should be at least equal to the essential order $\overline{\alpha}_{\mathrm{R}i}$ of the output y_i

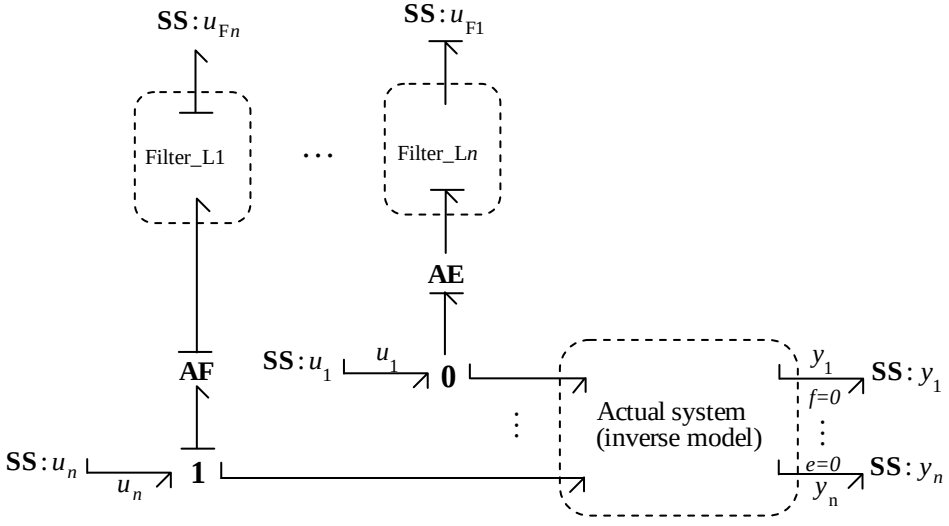

Fig. 2 Left filtered inverse bond graph configuration (for the actual system, u_1 and y_1 are assumed to be effort variables while u_n and y_n are assumed to be flow variables). Relative degree $\rho_{\mathrm{L}i}$ of Filter_L*i* should be at least equal to the essential order $\overline{\alpha}_{\mathrm{L}i}$ of the output u_i

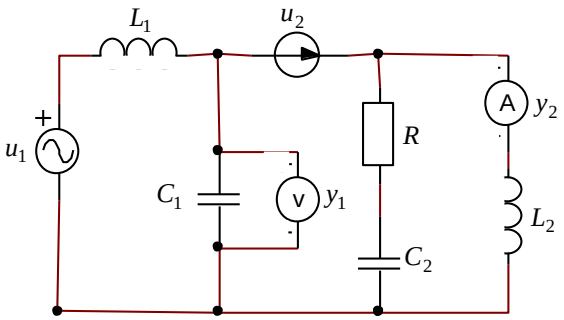

Fig. 3 An electrical circuit example

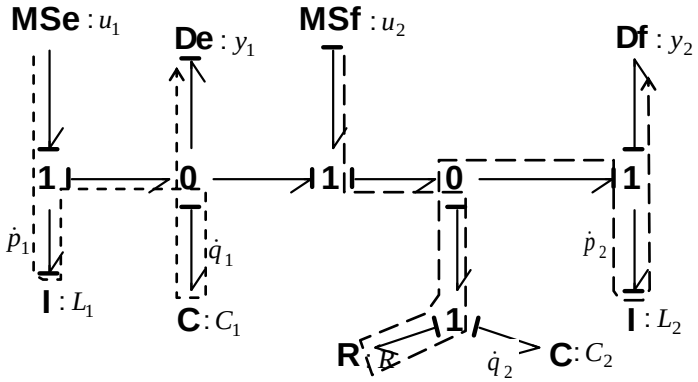

Fig. 4 Forward bond graph model of the electrical circuit in Fig. 3 with minimal length disjoint input-output causal paths indicated

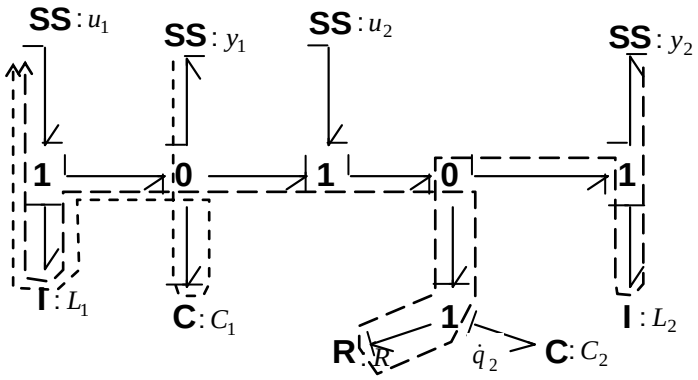

Fig. 5 Inverse bond graph model of the electrical circuit in Fig. 3 with highest order output-input causal paths indicated

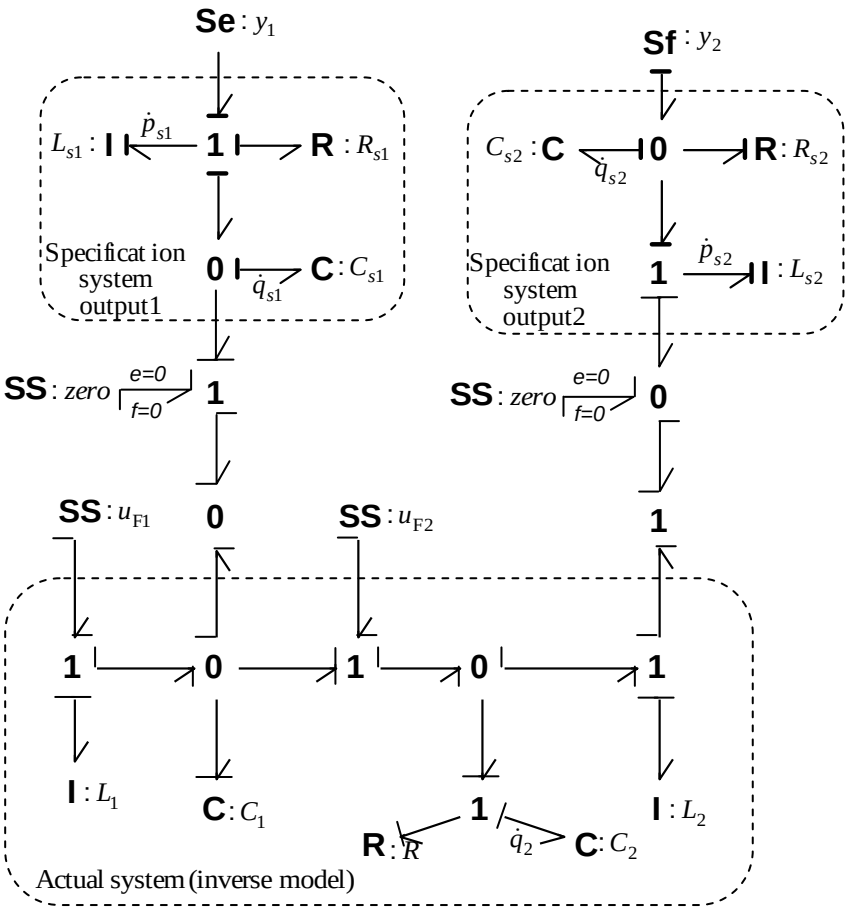

Fig. 6 – Right filtered inverse model configuration

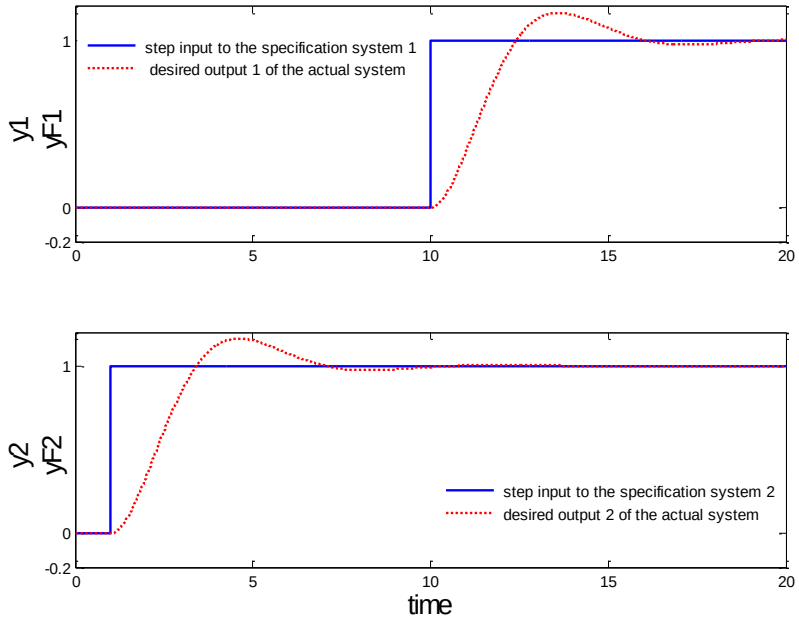

Fig. 7 – Right filtered inverse simulation results: step inputs y_1 and y_2 to the Filters or specification systems and resulting prescribed outputs y_{F1} and y_{F2} for the actual system

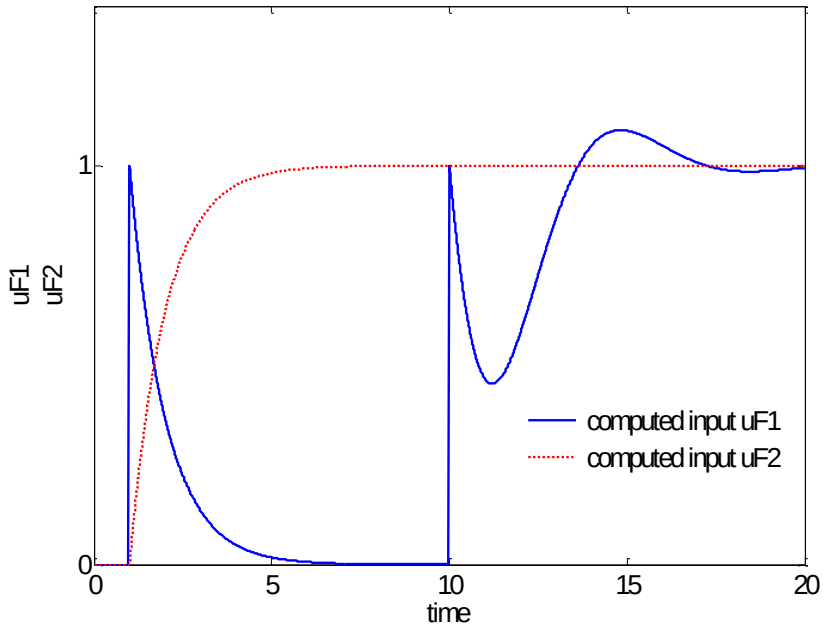

Fig. 8 – Right filtered inverse simulation results: computed inputs u_{F1} and u_{F2} to be applied to the actual system in order to achieve the desired filtered outputs y_{F1} and y_{F2} in Fig. 7

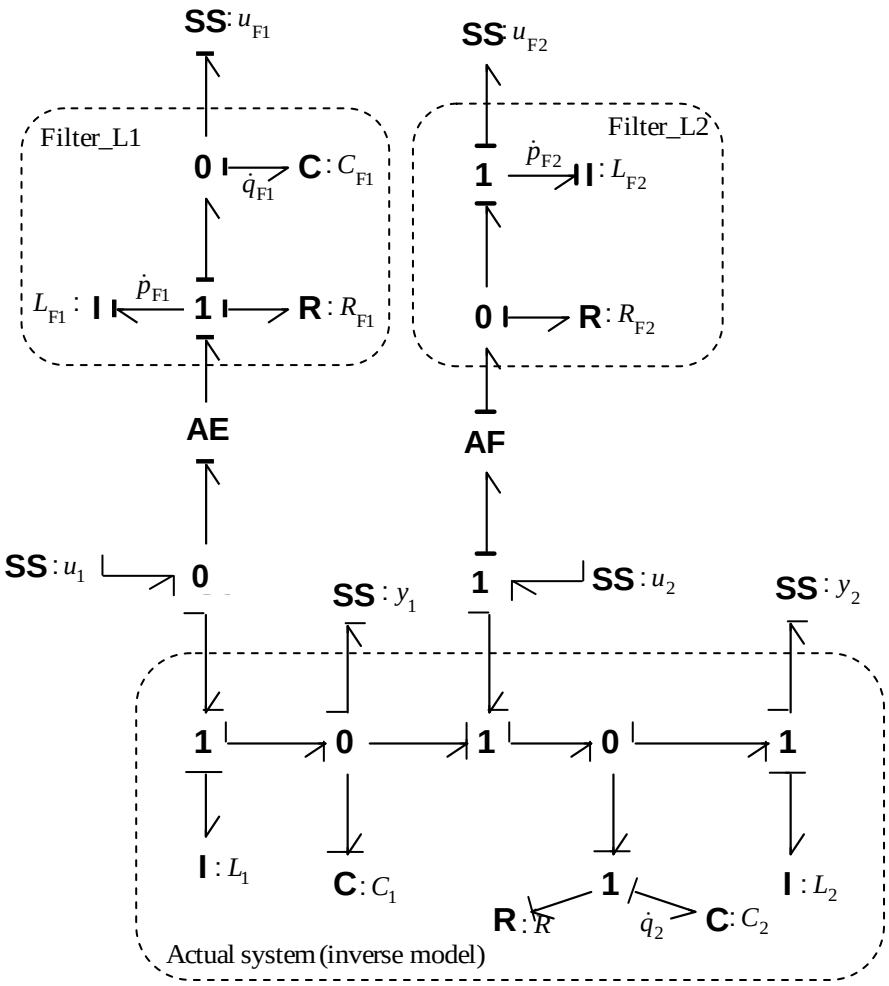

Fig. 9 – Left filtered inverse model configuration

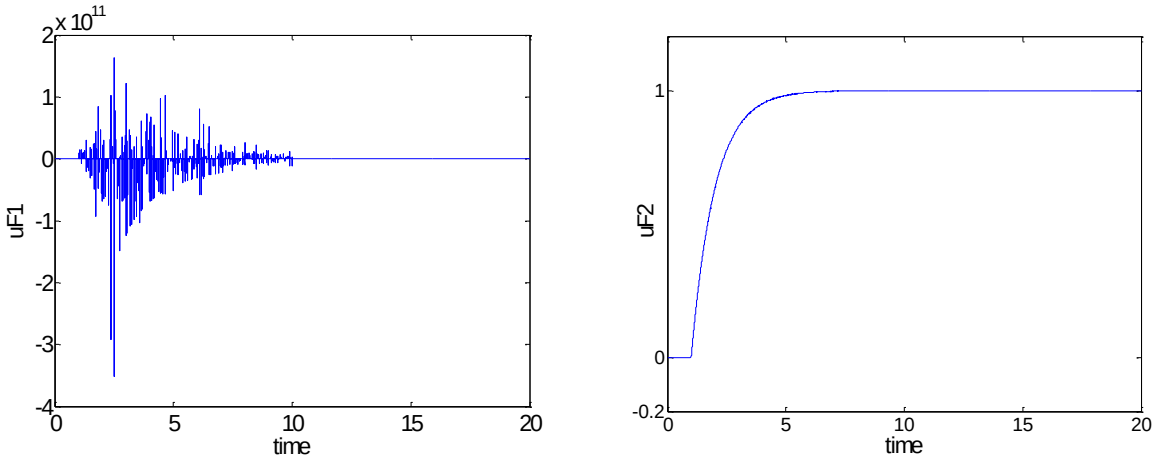

(a) (b)

Fig. 10 – Response of the exact inverse model cascaded with the actual system to reconstruct the inputs (with all parameters set to one) – (a) Reconstruction of input u_{F1} and (b) Reconstruction of input u_{F2}

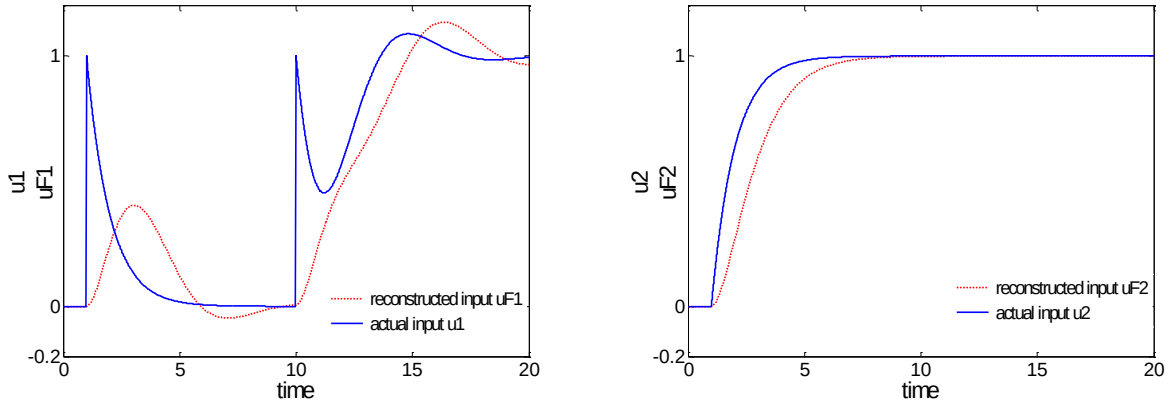

(a) (b)

Fig. 11 – Response of the left filtered inverse cascaded with the actual system to reconstruct the inputs (with all parameters set to one) – (a) Reconstruction of input u_{F1} and (b) Reconstruction of input u_{F2}

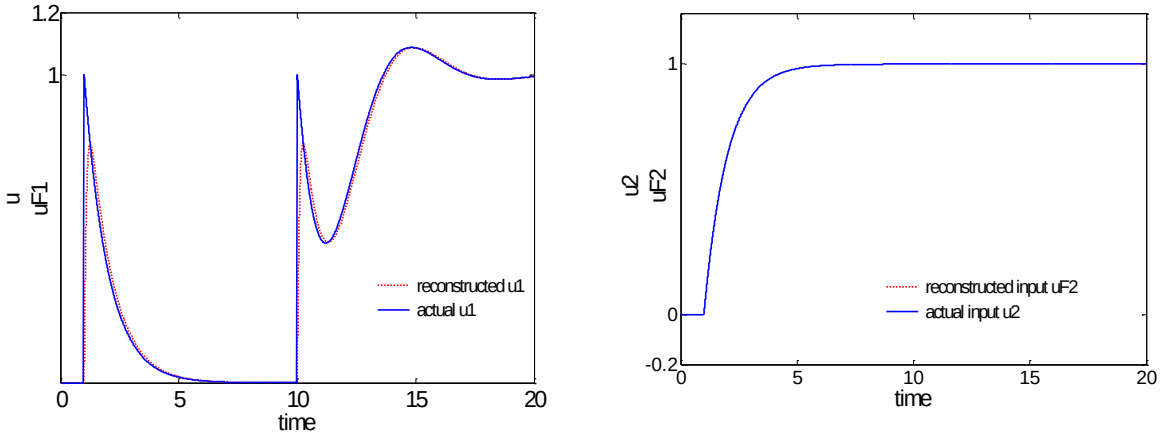

(a) (b)

Fig. 12 – Response of the left filtered inverse cascaded with the actual system to reconstruct the inputs (with parameters given in Table 1) – (a) Reconstruction of input u_{F1} and (b) Reconstruction of input u_{F2}